IEEE Access
Multidisciplinary ⋮ Rapid Review ⋮ Open Access Journal

Received August 18, 2020, accepted August 27, 2020, date of publication September 7, 2020, date of current version September 22, 2020.

Digital Object Identifier 10.1109/ACCESS.2020.3022505

Long Short-Term Memory Approach to Estimate Battery Remaining Useful Life Using Partial Data

BENVOLENCE CHINOMONA[1], (Graduate Student Member, IEEE), CHUNHUI CHUNG[1], (Member, IEEE), LIEN-KAI CHANG[1], WEI-CHIH SU[2], AND MI-CHING TSAI[1], (Senior Member, IEEE)

[1]Department of Mechanical Engineering, National Cheng Kung University, Tainan 701, Taiwan
[2]National Center for High-Performance Computing, National Applied Research Laboratories, Hsinchu 300, Taiwan

Corresponding author: Chunhui Chung (chchung@mail.ncku.edu.tw)

This work was supported by the Ministry of Science and Technology of Taiwan under Grant MOST 108-2622-8-006-014.

ABSTRACT Due to the increasing demand of electrical vehicles (EVs), prognostics of the battery state is of paramount importance. The nonlinearity of the signal (e.g. voltage) results in the complexity of analyzing the degradation of the battery. Aging characteristics extracted from the voltage, current, and temperature when the battery is fully charged/discharged were commonly used by previous researchers to determine the battery state. The drawbacks of the previous prediction algorithms are insufficient or irrelevant features to explicitly model the battery aging and the use of fully charged/discharged datasets, which might result in poor prediction accuracy. Therefore, this study proposes a feature selection technique to adequately select optimum statistical feature subset and the use of partial charge/discharge data to determine the battery remaining useful life (RUL) using Recurrent Neural Network – Long Short-Term Memory (RNN-LSTM). The proposed approach demonstrated exceptional RUL prediction results, with the root mean square error (RMSE) of 0.00286 and mean average error (MAE) of 0.00222 using partial discharge data. The proposed method shows prediction improvement in comparison with the use of full data and state-of-the-art outcomes from previous studies of the same open data from the National Aeronautics and Space Administration (NASA) prognostic battery data sets.

INDEX TERMS Recurrent neural network, long short-term memory, remaining useful life, battery management systems, feature selection.

I. INTRODUCTION

Considering the high threat of increasing global warming due to unprecedented environmental pollution caused by the use of fossil fuel, the need to use clean energy has gained great attention. Electric vehicles (EVs) have emerged as the uttermost environmentally friendly solution to tackle problems caused by fossil fuels. This resulted in steep demand for EVs, and there were over 7.2 million EVs deployed around the world by the end of 2019. The sales of electric cars topped 2.1 million globally and accounted for 2.6% of global car sales in 2019 indicating a continuous and rapid shift toward EVs popularity and use [1].

The lithium-ion (Li-ion) battery is widely used in electric vehicles because of its exceptional high cell voltage, high energy density, electromotive force, high output voltage, long lifetime, high charging efficiency, low self-discharge, low voltage drop, easy maintenance, and recycle [2]–[4]. These advantages have contributed to wider applications of lithium-ion batteries in more areas such as vehicles, household equipment, communications, aerospace, and other fields [5]. Even though there are noticeable advantages, aging is the most drawback of most lithium-ion batteries. After repeated cycling, the Li-ion cells are degraded and this affects the cell energy storage and output power capability [6]. The performance reduction of the battery in terms of cycle life can be greatly accelerated by overcharging, deep discharging, or operating the lithium-ion battery at elevated temperatures [7]. The capacity gradually deteriorates whether the battery is in use or not, eventually leading to failure. In the case of self-driving EVs, the capacity loss induces an autonomy reduction [8]. Thus, accurate estimation of the battery

The associate editor coordinating the review of this manuscript and approving it for publication was Xiao-Sheng Si.

capacity degradation is essential to avoid safety risks and provide reliable information that helps in prior maintenance planning and timely replacement of the battery.

Management of the battery life is of key importance in achieving highly efficient EVs. The remaining useful life (RUL) is a key parameter for scheduling repairs, evaluating the battery state, increasing the safety, and reducing accidents by providing an alarm before faults reach critical levels [9], [10]. The RUL is the useful life left at a particular time of operation or available service time left before the capacity reaches an unacceptable level [10]. The battery RUL is measured by the remaining number of charge and discharge cycles for the given battery. Currently, the model-based and data-driven methods are two techniques that are mostly used to predict the lithium-ion battery RUL. Model-based prognostics require a deep understanding of the composition of the model, in which mathematical expressions are used to describe the complex electrochemical process [11]. Goud *et al.* [7] developed a mathematical model to estimate the RUL of single cell Li-ion battery by considering the DC resistance during usage. However, the method can only be applied at the determined operating temperature with predetermined constants K1 and K2 (capacity loss when the battery is charged and discharged at different temperature conditions) and the RUL accuracy greatly decreases with the increase of the predicted cycles. Zhang *et al.* [12] used the F-distribution particle filter and kernel smoothing algorithm to predict the RUL. Their results indicated improved applicability and robustness by dynamically adjusting the particle weight in the prediction stage, thus realizing the battery RUL prediction. Even so, there is no evidence to suggest that the model can be applied to various working conditions such as high temperatures. The RUL prediction approach for lithium-ion batteries using Kalman filter and an improved particle filter (combining Kalman filter and particle swarm optimization) was conducted by Mo *et al*. [13]. The method not only improves the precision over standard particle filter but also overcomes the particle degradation due to particle resampling. Even though the results indicate better accuracy compared to particle filter (PF), the addition of the particle swarm optimization algorithm to solve the problem of particle degeneracy due to the resampling method further increases the complexity of the mathematical model. Other model-based methods were carried out such as Wiener Processes, sliding-window grey model, etc. [14]–[16].

Despite some success of model-based methods, in practice, it is difficult to have a precise and well-established model that would allow tuning and updating the parameters during the prediction phase with different operational conditions [17], and there are not well-established failure physical models [3]. Considering the above-mentioned drawbacks of model-based approaches to predict the RUL, data-driven methods have proven to be more efficient because there is no need for mathematical modeling to compute the battery degradation. Besides, the development of battery-related technology has increased, and more data on the energy storage devices have been produced. This facilitated the implementation of a data-based approach to estimate the RUL using accumulated historical data. The data-driven approaches can achieve simple noncomplex prediction of lithium-ion battery aging characteristics with acceptable accuracy. Li *et al*. [18] used a grey support vector machine (GSVM) to predict the RUL of the Li-ion battery and obtained 3.18% mean square error. Xu *et al.* [14] introduced a novel data-driven approach for lithium-ion battery RUL using an improved exponential model particle filter. The results showed that the capacity fade can be well captured.

Amongst the many data-driven methods to analyze the RUL, recurrent neural network (RNN) using long short-term memory (LSTM) cells emerged more powerful due to the ability to avoid the vanishing problem in gradient descent by learning long-term dependency (remember information for long periods) of capacity degradation tendencies for different conditions. The LSTM approach was utilized by Choi *et al.* [20] using a multi-channel charging profiles approach to estimate the remaining capacity. The prediction performance indicated a better prediction accuracy of the LSTM model compared to the feedforward neural network (FNN) and convolutional neural network (CNN). Zhang *et al.* [21] proposed LSTM to synthesize a data-driven RUL applying the Monte Carlo (MC) simulation to generate RUL prediction uncertainties. The required training data was 20-50% less using LSTM compared to particle filter (PF), and the performance results indicated that the LSTM generally predicts more accurate and precise than the support vector machine (SVM) and simple recurrent neural networks (SimRNNs). Park *et al.* [3] compared LSTM method with basic RNN, gated recurrent unit (GRU) and simple recurrent unit (SRU) using multi-channel charging profiles, and the mean absolute percentage error (MAPE) of the LSTM was better than basic RNN, GRU, and SRU by 32-52%.

This study adopted the LSTM method due to its superiority in predicting the RUL because it presents better performance compared to other models. However, effective feature extraction from the raw signals is crucial in estimating the RUL of the battery. The drawbacks of the previous LSTM algorithms are insufficient or irrelevant features to explicitly model the battery aging. In this study, a forward selection-long short-term memory (FS-LSTM) technique was developed to adequately select an optimum feature subset by disregarding irrelevant features for faster computation and better prediction. In addition, the effective data range from the charging/discharging signals was studied. The results show that predictions of the RUL perform much better with the partial data. The remaining sections are structured as follows: Section II briefly describes the LSTM architecture and RUL computation. In section III, data preprocessing is considered whereby the lithium-ion battery experiments are explained and the statistical methods used to extract the relevant features are given. The proposed FS-LSTM algorithm and partial charging/discharging data selection are introduced in section

IV. Section V presents the results and discussion. Finally, the conclusions are given in section VI.

II. ESTIMATION OF BATTERY REMAINING USEFUL LIFE

A. LONG SHORT-TERM MEMORY

The LSTM introduced by Hochreiter and Schmidhuber [22] in 1997 is a unique type of RNNs. The traditional RNN takes one or more inputs and produces one or more output vectors. The basic RNN is not capable of learning long term dependencies and mostly results in the vanishing gradient problem. The LSTM, however, was introduced to solve this problem with the ability to map the input to the output vector while remembering the information for a long duration of time. The LSTM uses memory cells as compared to hidden nodes in ordinary RNN. The cell state c_t is the basis of the LSTM method.

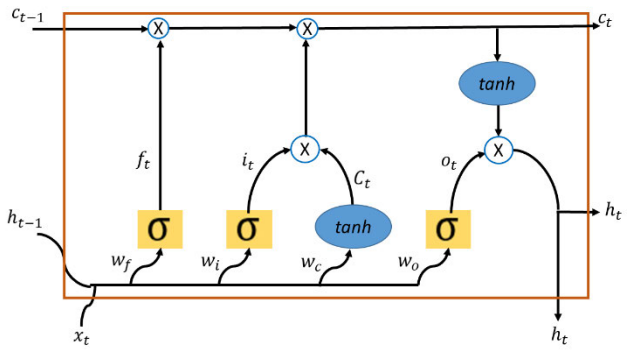

FIGURE 1. The basic architecture of the LSTM.

Figure 1 shows the basic architecture of the LSTM. The charging/discharging datasets of the battery are regarded as long-term time-series data; thus, the LSTM can learn the long-term dependency of the degradation data of the capacities and predict the lithium-ion battery's RUL [23]. The LSTM consists of three special gates, namely the forget (f_t), input (i_t), and output (o_t) gates. These carefully regulated structures (gates) can optionally decide what information should pass through [21]. The current input (x_t) and output from the previously hidden layers (h_{t-1}) at each step are used to compute the output with the respective weights (i.e. forget gate weight (w_f), input gate weight (w_i), input node weight (w_c), and output gate weight (w_o)), biases, the state activation functions (*tanh*), and gate activation functions (σ).

The forget gate controls the internal recurrent. It determines the information from the previous output (c_{t-1}) that will be discarded, updated, and stored. The forget gate is computed as:

$$f_t = \sigma\left(w_f[h_{t-1}, x_t] + b_f\right) \tag{1}$$

The input gate determines the information passed to the cell state. It contains the sigmoid activation function (σ) that regulate the information to be updated and a hypertangent activation function (*tanh*) that generates a new vector ($\tilde{c_t}$) that is added to the cell state. The input gate is calculated as:

$$i_t = \sigma\left(w_i[h_{t-1}, x_t] + b_i\right) \tag{2}$$

$$\tilde{c}_t = \tanh\left(w_i[h_{t-1,}x_t] + b_c\right) \tag{3}$$

The new cell state value (c_t) is obtained by multiplying the previous output (c_{t-1}) with the output of equation (1) and combining with the product of (2) and (3) as:

$$c_t = i_t \times \tilde{c}_t + f_t \times c_{t-1} \tag{4}$$

The output gate uses the sigmoid activation function and determines the output information. The output gate is calculated as:

$$o_t = \sigma\left(w_o[h_{t-1}, x_t] + b_o\right) \tag{5}$$

The hidden state (h_t) can finally be computed by passing the cell state (c_t) through the activation function, *tanh*, and multiplying with the output of the output gate [21]:

$$h_t = o_t \times \tanh\left(c_t\right) \tag{6}$$

B. ESTIMATION OF REMAINING USEFUL LIFE

The remaining useful life of a battery is described as the actual remaining cycles before the given specific end of life, which is usually defined by the critical degraded capacity. Assuming that α is the current number of charge/discharge cycles, and β is the number of cycles estimated at the end-of-life (EOL). By predicting the EOL cycles, we can get the battery RUL as follows [24]:

$$RUL = \beta - \alpha \tag{7}$$

The RUL is closely related to battery capacity and internal resistance. The complex aging mechanisms and the high cost of measuring the internal parameters of the battery make the use of internal resistance difficult in practical engineering [24]. However, the data-driven models have been developed using those accessible signals. Therefore, in this study, the relationship between capacity and the operating conditions such as terminal voltage, current, and temperature is employed to estimate the RUL. The RUL error is calculated as the difference between the actual and predicted remaining cycles:

$$RUL_{error} = RUL_{predicticted} - RUL_{actual} \tag{8}$$

The capacity was calculated by integrating the current over time:

$$C_{Ah} = \int_{t_o}^{t_1} I(t)dt \tag{9}$$

where t_o is the start of charge/discharge of each cycle, t_1 is the end of charge/discharge, and $I(t)$ is the corresponding current.

TABLE 1. Specifications of the battery datasets.

Battery type	Maximum charging	End of discharge	Battery number	No. of cycles
Li-ion	4.2V	2.7V	B0005	168
		2.5V	B0006	168
		2.2V	B0007	168
		2.5V	B0018	132

III. DATA PREPROCESSING

To achieve a better estimation of battery RUL, the inputs of the model were extracted from the battery charge/discharge data. Two steps of LSTM model training were conducted. In the first step, the raw data was preprocessed into different features. Different combinations of the features were tested as the inputs, and the performance was compared to find out the best combination of the inputs. In the second step, only part of the data within specified ranges were utilized in the model training. The results show that the utilization of partial data performs better than the use of the full data.

A. DATA

The lithium-ion battery datasets were obtained from NASA Prognostic Center of Excellence [25]. A constant current and constant voltage principles were used to charge and discharge the batteries. Charging was carried out at 1.5 A until the maximum voltage of 4.2V, then constant voltage was controlled until charging current drop to 20mA. Discharging was carried out at 2 A until the cut of voltage for the specified batteries as listed in Table 1. The capacity of 1.4 Ah was considered as the end of life (EOL), which is 30% decrease of the initial rated capacity of 2Ah. The battery signals of terminal voltage, output current, time, and temperature were retrieved from battery No. 5, 6, 7, and 18.

Figure 2 shows the experimental discharge voltage, current, and temperature signals of battery No. 5. The current goes to negative because it flows out of the battery at the initial discharge. The battery voltage and temperature significantly changed with time during the discharging process. The voltage decreases, while the temperature increased due to several sources, such as electronic circuit elements located around the battery conducting heat into the cells, waste heat including protection, and gas gauge circuits inside the battery itself. Thus, the signal dynamics can be utilized to characterize distinctive features and estimate the remaining useful life.

B. FEATURE EXTRACTION

Feature extraction can be described as the reduction process whereby meaningful attributes are extracted from the raw signals to reduce the dimensionality without compromising the properties of the input data patterns. In this study, statistical methods were used to extract the relevant features. The

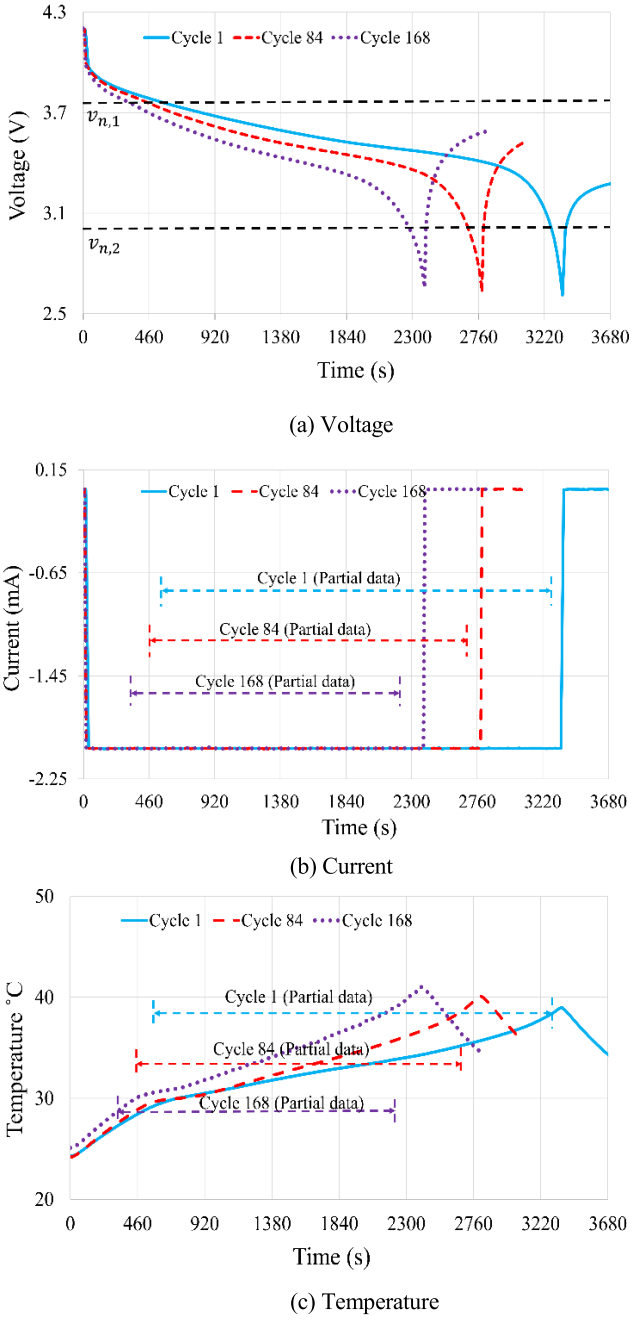

FIGURE 2. Discharge voltage, current, and temperature signals of battery No. 5 and partial data extracting range ($v_{n,1}$, $v_{n,2}$).

capacity degradation is affected by many factors such as loading, temperature, humidity, cyclic life, depth of discharge, recharge rate, etc. It is practically difficult to consider all these factors. Therefore, the voltage, current, and temperature signals were considered in this study. A total of 18 features were extracted from the data. These features include energy signal, mean, power signal, standard deviation, skewness, and kurtosis of the signals in each cycle. The statistical features are computed as shown in equation (10)-(15).

The energy signal (e_j) is calculated by taking the integral of the magnitude square of the input signals (x_i) from the initial charging/discharging time (t_o) to the end of charge/discharge (t_1) in each cycle:

$$e_j = \int_{t_0}^{t_1} |x_i|^2 \, dt \tag{10}$$

where j represents the voltage, V, current, C, or temperature, T.

The power signal (p_j) is the natural logarithm of the average energy over time, which is calculated as:

$$p_j = In\left(\frac{1}{T}\int_{t_0}^{t_1} |x_i|^2 \, dt\right) \tag{11}$$

The mean of the signals represented by m_j is the average of the signals in each cycle.

$$m_j = \frac{1}{n}\sum_{i=0}^{n} x_i \tag{12}$$

To compute the standard deviation, the sum of the square of the deviation between x_i, and m_j is taken before computing the average. The square root is used to compensate for the initial squaring:

$$d_j = \sqrt{\frac{1}{n}\sum_{i=0}^{n} \left(x_i - m_j\right)^2} \tag{13}$$

The skewness and kurtosis features are calculated similarly to standard deviation, but the cubic and quadruple of the differences between x_i, and m_j are taken before the average and divided by their respective standard deviation power:

$$s_j = \sqrt{\frac{1}{n}\sum_{i=0}^{n} \frac{\left(x_i - m_j\right)^3}{d_j^3}} \tag{14}$$

$$k_j = \sqrt{\frac{1}{n}\sum_{i=0}^{n} \frac{\left(x_i - m_j\right)^4}{d_j^4}} \tag{15}$$

The features were in different units and scales. Therefore, the signals were transposed to the data range between 0 and 1. The input/target data was normalized prior to training and testing processes. This is crucial to obtain good results by reducing the complexity of the data structure. However, the model performance was carried out using the denormalized predicted capacity output of the test cycles and the measured experimental capacity. The normalization was conducted on each battery dataset.

$$\overline{x_i} = \frac{f_i - \min f_i}{\max f_i - \min f_i} \tag{16}$$

where f_i is the input feature and $\bar{x}_i$ represents the normalized input feature.

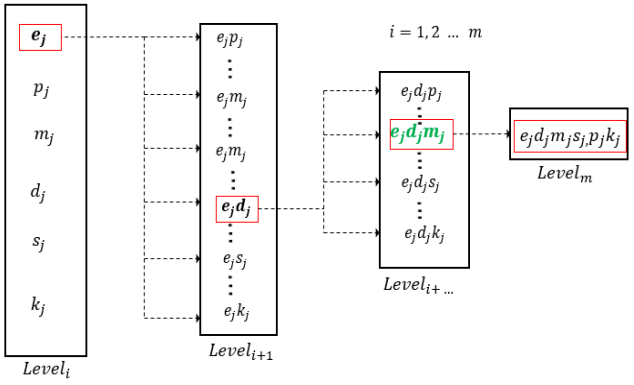

FIGURE 3. Proposed forward feature selection algorithm.

IV. FORWARD SELECTION ALGORITHM AND STUDY ON PARTIAL DATA

A. FS-LSTM ALGORITHM

Feature selection has a great impact on the performance of the model. The forward feature selection method was implemented to choose a distinctive feature subset that can successfully describe the deterioration of the battery cells. Figure 3 shows the feature selection algorithm, whereby initially all the 18 features were evaluated separately as the input of the LSTM model. In the second level, the algorithm used the previously selected best subset to iterate all possible combinations with one of the remaining features, and so on. Therefore, one feature was added to the selected feature subset based on the evaluated performance in each level. A total of 170 possible feature combinations were evaluated and the global best feature subset was chosen to model lithium-ion battery degradation. This feature selection method significantly reduces the number of evaluations during the feature selection process.

B. STUDY OF PARTIAL DATA

The estimation of RUL has mostly been conducted using charge/discharge signals considering battery datasets containing full charge/discharge data. However, the use of charge or discharge data in a full cycle includes insignificant signals and increases computational time. Within a specific range, the signal can accurately determine the capacity loss. This can be due to the elimination of highly fluctuating signals at the initial and the end of charge/discharge which might result in poor model performance. Therefore, the performance of partial signals to estimate the RUL was investigated in the second step of this study.

To select partial data, this study considered the voltage range as the benchmark for the extraction of partial datasets. Thus, the voltage range of $v_{n,1}$ to $v_{n,2}$ was selected, where $v_{n,1}\mathrm{v_{n,1}}$ represents the upper limit of the selected voltage, and $v_{n,2}\mathrm{v_{n,2}}$ is the low limit. Different partial data such as current, time, and temperature were selected in correspondence to the voltage range. Figure 2 shows the selected partial discharge data (3.8 – 3.0 V) for cycles 1, 84, and 168. It can be noted

that the current and temperature samples are selected in the same given period based on the defined voltage range. This allows the extraction of features from all the cycles based on the same standard and provides the battery degradation phenomena without compromising the total number of cycles of the original data.

In this study, the capacity was used as the RUL indicator. The flowchart of the proposed method to predict the RUL of the lithium-ion battery is represented in Fig. 4. In summary, features were extracted from voltage, current, and temperature signals. Capacity was used as the target class and data was normalized before training and testing. The input features were selected using the forward selection method. The selected global best feature subset f_s was used as the input of the LSTM model to predict the RUL.

V. RESULTS AND DISCUSSION

In this study, the LSTM architecture was carried out using the LSTM Toolbox in Matlab 2019a. The layer specifications for training the model includes the input size corresponding to the number of the features and 50 hidden layers with a fully connected layer. Adam optimizer with 0.001 learning rate, 500 epochs, and a batch size of 50 was used.

Root mean square error (RMSE) and mean absolute error (MAE) were used to evaluate the performance of the trained model considering the difference between the actual and denormalized predicted capacity after each discharge cycle in the whole battery life.

$$RMSE = \sqrt{\frac{1}{n}\sum_{i=1}^{n}\left(\left|x_a - x_p\right|\right)^2} \tag{17}$$

$$MAE = \frac{1}{n}\sum_{i=1}^{n}\left|x_a - x_p\right| \tag{18}$$

where x_p and x_a are the predicted and actual capacities, respectively.

A. PERFORMANCE OF FS-LSTM METHOD

In the first step, the full charge and discharge data in each cycle were calculated into the features as the inputs of the LSTM model. Feature selection is essential because the RUL prediction depends on the accuracy of the training model. The extracted 18 features were used as the input data to train the model. The performance of different feature subsets was evaluated based on the forward feature selection method presented in section IV. Battery No. 5 dataset was used to test the trained model and perform feature selection. The other three battery datasets (No. 6, 7, and 18) were used for model training.

Tables 2 and 3 indicate the 10 best performance feature subsets based on the results of MAE using charge and discharge data, respectively. The results clearly show the importance of feature selection to yield a minimum error. When insufficient or irrelevant features are selected, the model performs poorly. It is indicated that the use of many features does not necessarily guarantee better performance. The model can perform better using only 3 or 4 features than the inputs with all the features. Therefore, the input data size can be significantly reduced, while the accuracy is increased by using the developed feature selection method.

TABLE 2. Top 10 testing performance of the feature subsets using charge dataset of battery No. 5.

RANK	FEATURE	RMSE	MAE
1	$e_v p_{v,c} m_{v,c} s_{v,c} k_t$	0.01498	0.01166
2	$e_v p_{v,c} m_c$	0.01638	0.01229
3	$e_v p_{v,c} m_{v,c}$	0.01632	0.01267
4	$e_v p_{v,c} m_{v,c} s_c$	0.01632	0.01270
5	$e_v p_{v,c} m_{v,c} s_{v,c}$	0.01671	0.01230
6	$e_v p_{v,c} m_{v,c} s_v d_c$	0.01592	0.01278
7	$e_v p_{v,c} m_{v,c} s_{v,c} d_v k_c$	0.00137	0.01289
8	$e_v p_{v,c} m_{v,c} s_v k_c$	0.01654	0.01302
9	$e_{v,t} p_{v,c} m_{v,c} s_{v,c} d_v k_{v,c}$	0.01717	0.01311
10	$e_{v,t} p_{v,c} m_v s_v$	0.01735	0.01313
	all	0.03549	0.03026

TABLE 3. Top 10 testing performance of the feature subsets using discharge dataset of battery No. 5.

RANK	FEATURE	RMSE	MAE
1	$e_{c,t} p_v m_v d_c s_c k_{c,t}$	0.00286	0.00222
2	$e_{c,t} p_v m_v k_c$	0.00287	0.00224
3	$e_{c,t} p_v$	0.00313	0.00245
4	$e_{v,c,t}$	0.00325	0.00246
5	$e_{c,t} p_v m_v k_t$	0.00332	0.00253
6	$e_{c,t} p_v m_v d_c$	0.00344	0.00275
7	$e_{c,t} p_v m_v k_{c,t}$	0.00358	0.00287
8	$e_{c,t} p_v m_v$	0.00358	0.00290
9	$e_{c,t} p_v k_t$	0.00372	0.00301
10	$e_{c,t} m_v$	0.00386	0.00308
	all	0.01195	0.01123

The obtained results from the feature selection algorithm (FS-LSTM) using charge and discharge dataset are compared to recent results. The state-of-the-art results used for comparison was presented by Choi *et al.* [20], where Multi Channel-Long Short-Term Memory (MC-LSTM) was applied, with an input matrix of a 30-dimensional vector of concatenated voltage, current, and temperature from charge data. The data from three batteries were used for model training and the remaining battery for testing. The performance error of 0.01946 RMSE and 0.01118 MAE was obtained using the proposed FS-LSTM algorithm with charge data, while MC-LSTM achieved 0.0246 RMSE and 0.0159 MAE for battery No. 18 [20]. The results of the proposed FS-LSTM using charge data indicate that the FS-LSTM algorithm selects features with relevant attributes to determine the battery aging phenomenon. However, the use of discharge data greatly improves the accuracy of the proposed FS-LSTM model.

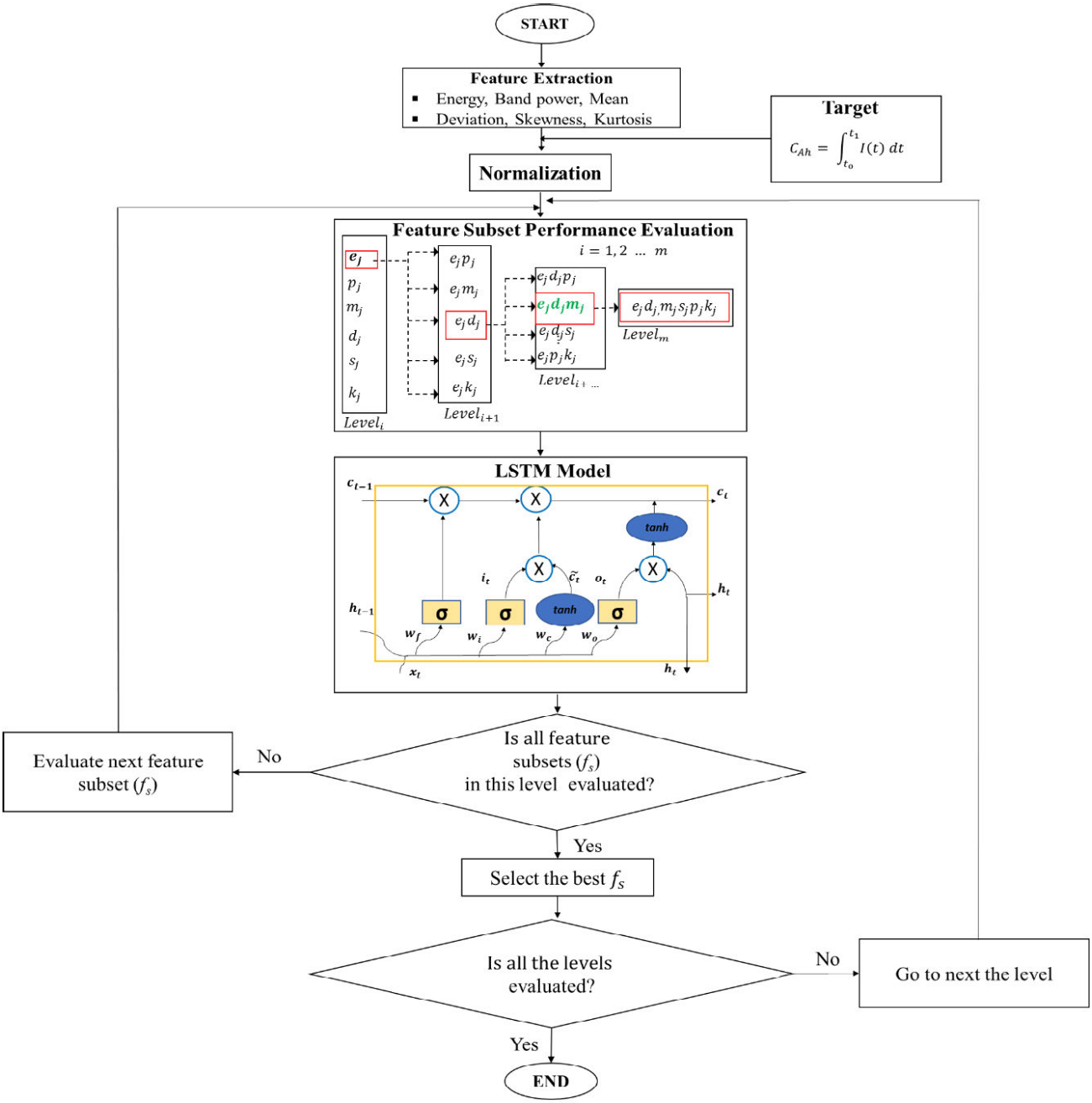

FIGURE 4. Flowchart of the proposed forward selection - long short-term memory method (FS-LSTM) for RUL prediction.

Figure 5 presents the results and an estimation of the battery capacity using charge and discharge data with the proposed feature selection algorithm. The results of the feature selection algorithm using discharge data perform much better than the charge data for all the batteries.

B. REMAINING USEFUL LIFE PREDICTION USING PARTIAL DATA

In the second step, the RNN-LSTM was used with partial charge/discharge data as the input and the measured capacity as the target to predict the RUL of the battery. The partial data was chosen considering the voltage range as the benchmark. The current and temperature was selected in correspondence to the voltage range as described in section III. The full charge and discharge data specifications were described in Table 1 for all the selected batteries. The RMSE and MAE were used to evaluate the performance considering the measured experimental capacity and predicted battery capacity values. The best performance of partial voltage ranges is listed in Tables 4 and 5. The partial range selection

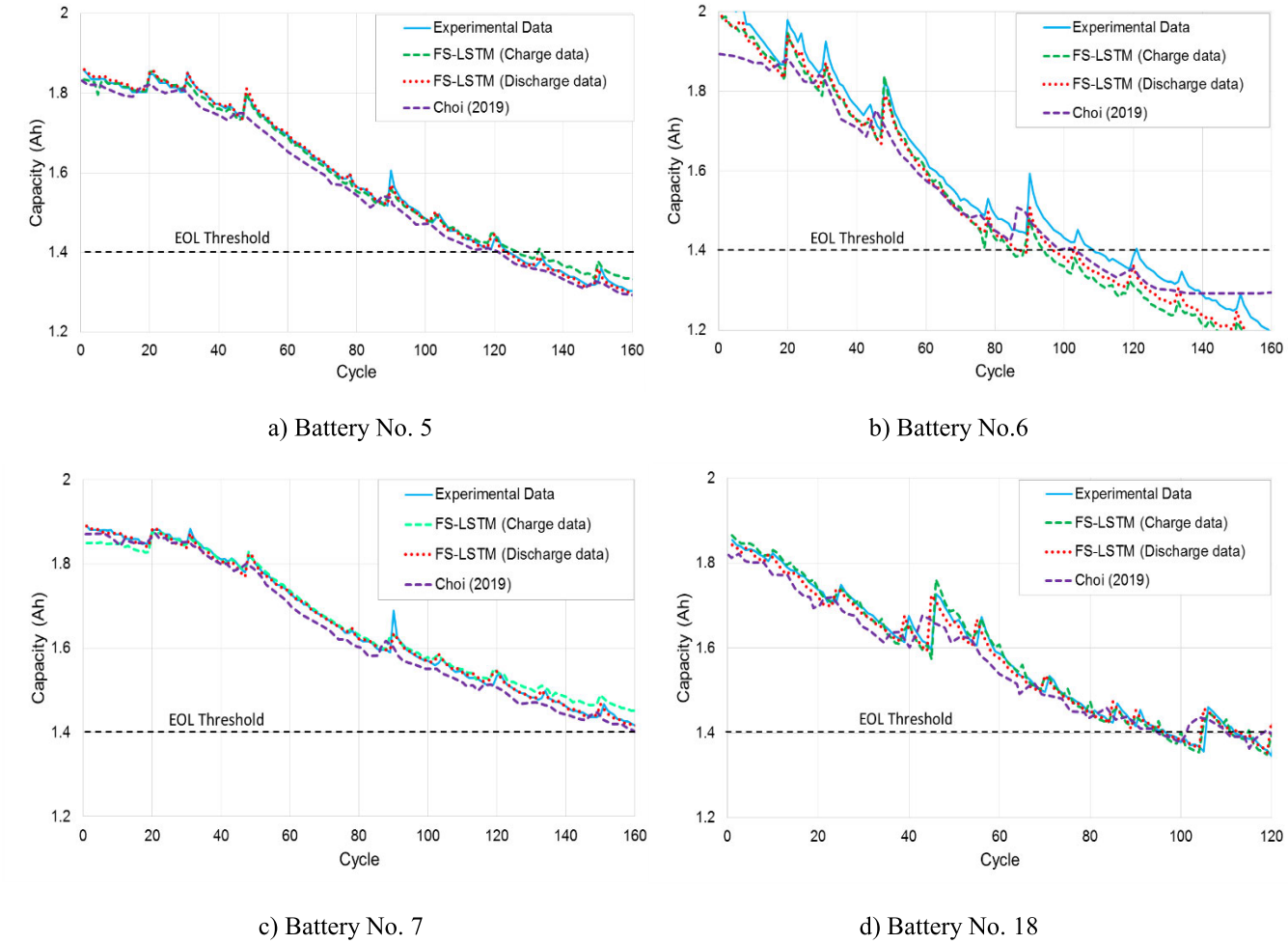

FIGURE 5. Comparison of the estimated capacity using the proposed FS-LSTM with charge/discharge data and multi-channel profile (MC-LSTM) [20]: (a) battery No. 5, (b) battery No. 6, (c) battery No. 7, and (d) battery No. 18.

is carried out using battery No. 5 with 50 cycles as the training datasets, and the remaining cycles were used to test the model.

The initial parameters were learning rate of 0.0001, 500 epochs, and a batch size of 10 using Adam optimizer. The results indicate that the best range of 3.6-4.2V and 4.0-3.1V greatly improve the performance of the FS-LSTM model compared to full charge and discharge data respectively. The RMSE of 0.13054 and MAE of 0.11911 were obtained using partial charge data, and RMSE of 0.06448 and MAE of 0.06125 were achieved using partial discharge data. The utilization of partial data performs much better than the full data as presented in Tables 4 and 5. However, the range of 3.6-4.2V does not represent all the cycles because in some cycles the initial charging starts at 3.8V. Therefore, the partial charge range of 3.8-4.1V was selected to perform the RUL. The study of the partial data range indicates that the use of the full data does not guarantee a better prediction accuracy. Improved performance by using partial data can be attributed to the minimum disturbance in the selected signal range as there are high fluctuations during the initial charging and discharging phases in the experiments.

TABLE 4. Performance of partial charge data with different voltage ranges.

	50 training cycles		
Battery	RANGE	RMSE	MAE
No. 5	**2.7 - 4.2**	**0.16140**	**0.14594**
	3.6 - 4.2	0.13054	0.11911
	3.8 - 4.1	0.13060	0.12080
	3.3 - 4.2	0.13460	0.12214
	3.5 - 4.1	0.13633	0.12319
	3.6 - 4.1	0.13622	0.12365
	3.4 - 4.2	0.13835	0.12571
	3.4 - 4.1	0.14109	0.12758
	3.7 - 4.2	0.13993	0.12855
	3.1 - 4.1	0.14280	0.12913
	3.7 - 4.0	0.14410	0.12922

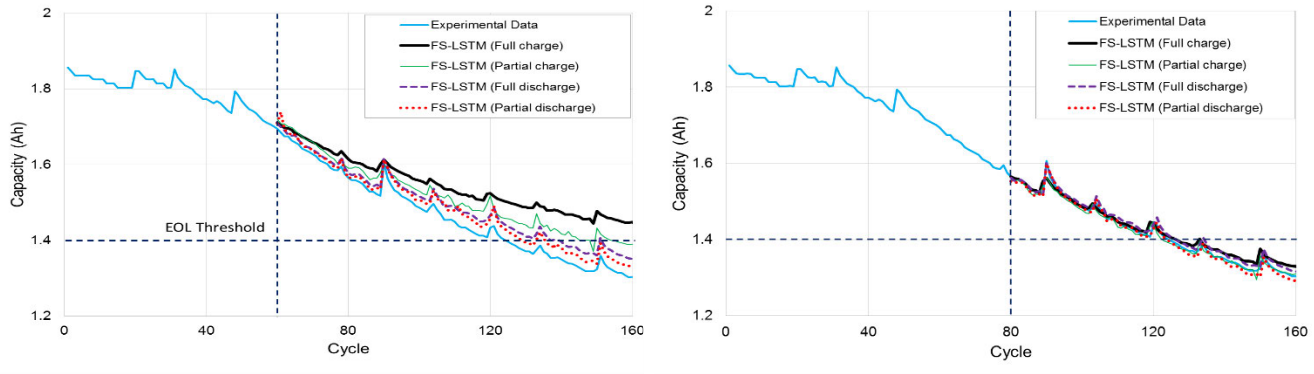

(a) Battery No. 5

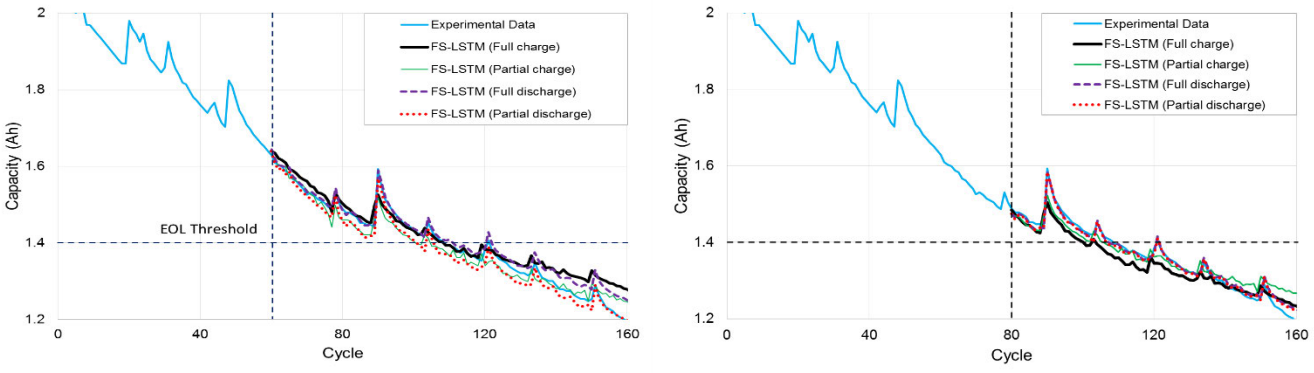

(b) Battery No. 6

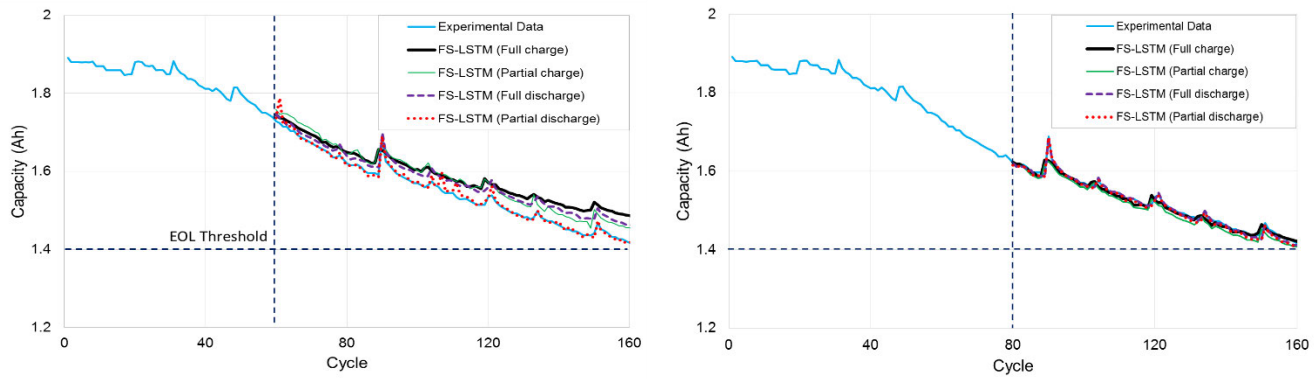

(c) Battery No. 7

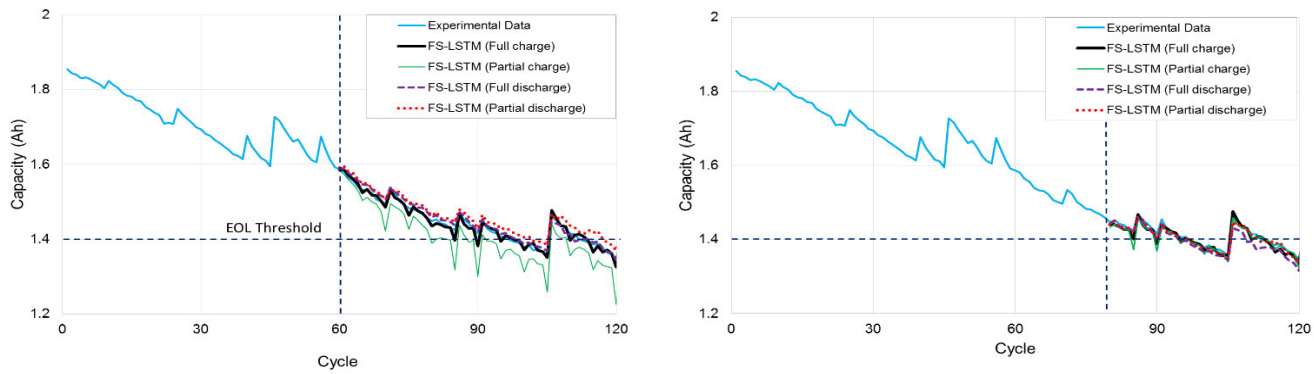

d) Battery No. 18

FIGURE 6. RUL prediction using full and partial charge/discharge data of (a) battery No. 5, (b) battery No. 6, (c) battery No. 7, and (d) battery No.

TABLE 5. Performance of partial discharge data with different voltage ranges.

Battery	50 training cycles RANGE	RMSE	MAE
No. 5	**4.2 - 2.7**	**0.09531**	**0.08817**
	4.0 - 3.1	0.06448	0.06125
	4.1 - 2.7	0.06468	0.06141
	4.1 – 3.0	0.06652	0.06311
	4.0 - 3.1	0.06801	0.06410
	3.6 - 3.2	0.07039	0.06747
	4.1 - 2.8	0.07201	0.06814
	4.0 - 3.3	0.07312	0.06865
	3.6 - 3.3	0.07349	0.06893
	4.0 - 3.0	0.07444	0.06981
	4.0 - 2.9	0.07471	0.07007

TABLE 6. RUL prediction performance using charge data.

Train Data	Battery No.	Full discharge data RMSE	Full discharge data MAE	Partial discharge data RMSE	Partial discharge data MAE
40 Cycles	5	0.19854	0.17725	0.17202	0.15651
	6	0.10986	0.09645	0.08647	0.07366
	7	0.14923	0.13651	0.13919	0.12837
	18	0.02380	0.02109	0.01969	0.01380
60 Cycles	5	0.09591	0.08714	0.05919	0.05476
	6	0.04162	0.03017	0.03306	0.02610
	7	0.04548	0.04209	0.03568	0.03432
	18	0.01129	0.00852	0.04632	0.04029
80 Cycles	5	0.01585	0.01176	0.01223	0.00956
	6	0.03445	0.02928	0.03854	0.02919
	7	0.01088	0.00694	0.01120	0.00798
	18	0.01029	0.00808	0.01355	0.00931

TABLE 7. RUL prediction performance using discharge data.

Train Data	Battery No.	Full discharge data RMSE	Full discharge data MAE	Partial discharge data RMSE	Partial discharge data MAE
40 Cycles	5	0.10238	0.09456	0.08405	0.07891
	6	0.08908	0.08215	0.05050	0.04515
	7	0.10250	0.09612	0.08739	0.08321
	18	0.02872	0.02591	0.05502	0.05120
60 Cycles	5	0.03696	0.03406	0.02599	0.02376
	6	0.03011	0.02792	0.01489	0.01043
	7	0.03293	0.03067	0.01012	0.00560
	18	0.00975	0.00842	0.02216	0.02075
80 Cycles	5	0.01226	0.01079	0.00809	0.00694
	6	0.01737	0.01200	0.01627	0.01174
	7	0.00562	0.00420	0.00722	0.00617
	18	0.01905	0.01696	0.00668	0.00573

Figure 6 illustrates the RUL performance using partial charge (3.8-4.1V), partial discharge (4.0-3.1V), and full charge/discharge data for battery No. 5, 6, 7, and 18. The training cycles of 40, 60, and 80 were utilized to evaluate the RUL for all the batteries. The capacity of 1.4 Ah was considered as the end of life (EOL), i.e. 30% decrease of the initial rated capacity of 2Ah. The results of the RMSE and MAE are listed in Tables 6 and 7 for charge and discharge data. When 40 cycles were used to train the model, it can be observed that the proposed model using partial data outperforms the use of full charge data. When 60 cycles were used to train the model, a similar trend of the error is observed with partial data outperforming full discharge data for battery No. 5, 6, and 7. The RUL prediction for battery No. 18 presents an increase in the error when partial charge data were used compared to the use of full charge data. However, when the training data were increased to 80 cycles, better RUL prediction was achieved. Both the proposed partial charge/discharge and full charge/discharge data presented excellent prediction accuracy as shown in Tables 6 and 7. Table 8 indicates the RUL error for battery 5, 6, and 18 using 60 and 80 cycles as the prediction starting point. The partial data has an excellent RUL prediction error, however, full charge data performed better on battery No. 18 in comparison with partial data. Fig. 6 shows the predicted results for all the selected batteries. Thus, the RUL prediction using partial data performs better or equal to the prediction using full discharge data, although the results converge with more cycles. In addition to better accuracy, the use of partial data can be of great significance in reducing the input size when a large amount of data is used for model training. Hence, the shorter training time and better performance of the model are expected.

To validate the performance of the selected partial range for both charge and discharge data, the results were compared to the results presented by Park *et al.* [3]. Table 9 and Fig. 7 shows the results of the proposed FS-LSTM using partial charge and discharge data and MC-LSTM. Both the partial charge and discharge results of the FS-LSTM outperform MC-LSTM for battery No.5, 7, and 18. However, the MC-LSTM has better accuracy for battery No. 6.

The shortcoming of the proposed partial range is that the selected range of 3.8-4.1V and 4.0-3.1V for charge and discharge data might not necessarily represent the best partial data range for battery No. 6, 7, and 18. This is observed with the results of battery No. 18, where the full charge and discharge data performs better than the partial data. The best partial charge/discharge ranges that represent each battery can be further investigated using the proposed algorithm, and a universal range for all the batteries would be selected to train the model. Thus, selecting the best range for all the batteries will provide a global partial charge/discharge range that can be generally applied to predict the RUL of all battery datasets with improved accuracy. The study of charge data also shows better performance than the state-of-the-art results [20], although it is not as good as the discharge data. Nevertheless, using charge data may be more practical because the battery is usually discharged non-continuous.

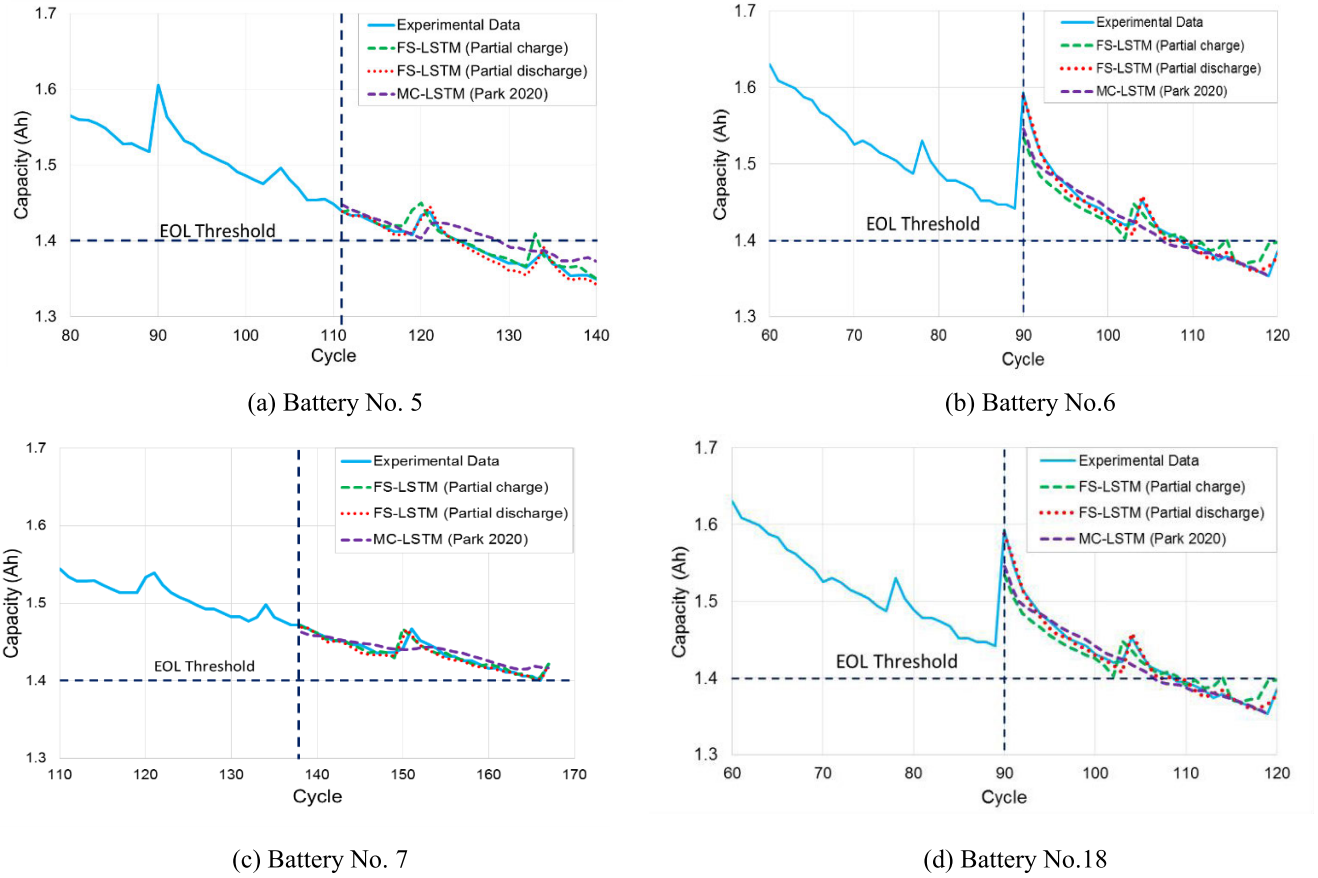

FIGURE 7. RUL prediction comparison of the proposed FS-LSTM with MC-LSTM [3].

TABLE 8. RUL errors of charge and discharge data.

Start Point	Battery No.		Full Charge		Partial Charge		Full Discharge		Partial Discharge	
		RUL_{act}	RUL_{pred}	RUL_{error}	RUL_{pred}	RUL_{error}	RUL_{pred}	RUL_{error}	RUL_{pred}	RUL_{error}
60	5	64	-	-	86	+22	81	+17	77	+13
	6	48	50	+2	46	-2	53	+5	47	+1
	18	36	39	+3	21	-15	40	+4	43	+7
80	5	44	48	+4	44	0	47	+3	46	+2
	6	28	25	-3	26	-2	29	+1	28	0
	18	12	16	+4	16	+4	16	+4	15	+3

TABLE 9. Comparison of the proposed FS-LSTM and MC-LSTM models.

Method	Battery No.5		Battery No.6		Battery No. 7		Battery No.18	
	RMSE	MAE	RMSE	MAE	RMSE	MAE	RMSE	MAE
FS-LSTM (charge)	0.0111	0.0073	0.0443	0.0328	0.0066	0.0045	0.0104	0.0084
FS-LSTM (discharge)	0.0091	0.0079	0.0197	0.0138	0.00401	0.0033	0.0057	0.0046
MC-LSTM (Park 2020 [3])	0.0168	0.0146	0.0152	0.0103	0.0085	0.0068	0.0388	0.0261

Since this study is limited to open access NASA data, more experiments have to be conducted to ascertain the validity of the developed feature selection algorithm and RUL prediction approach using partial charge/discharge data. Also, extensive analysis of the training time difference between the full and partial charge/discharge data can be studied to investigate the tradeoff between computation time and accuracy.

VI. CONCLUSION

A forward feature selection algorithm was developed in this study to select the best feature subset for better prediction accuracy of the remaining useful life of lithium-ion battery using the RNN-LSTM model. The algorithm effectively selects a significant feature subset which results in high accuracy of RUL prediction using charge/discharge data. In addition, the use of partial charge/discharge datasets to predict the battery RUL performs equal or better than the full data. To further ascertain the superiority of the model, better capacity prediction accuracy was achieved compared to the state-of-the-art results. The results in this study indicate that the feature selection method and the use of partial data can reduce the number of inputs and the amount of data to be processed, while the prediction accuracy is increased. Although the performance of the charge data is not as good as that of the discharge data, it may be more applicable in practical usage. This study is limited to the open access battery charge/discharge data. The robust feature selection and partial data range could be decided with more relevant data.

REFERENCES

[1] IEA, Paris, France. *Global EV Outlook 2020*. Accessed: Jul. 18, 2020. [Online]. Available: https://www.iea.org/reports/global-ev-outlook-2020

[2] P. Venugopal and T. Vigneswaran, "State-of-health estimation of lithium batteries in electric vehicle using IndRNN under variable load condition," *Energies*, vol. 12, no. 22, pp. 1–29, Nov. 2019.

[3] K. Park, Y. Choi, W. J. Choi, H.-Y. Ryu, and H. Kim, "LSTM-based battery remaining useful life prediction with multi-channel charging profiles," *IEEE Access*, vol. 8, pp. 20786–20798, Jan. 2020.

[4] J. C. A. Anton, P. J. G. Nieto, C. B. Viejo, and J. A. V. Vilan, "Support vector machines used to estimate the battery state of charge," *IEEE Trans. Power Electron.*, vol. 28, no. 12, pp. 5919–5926, Dec. 2013.

[5] L. Ren, L. Zhao, S. Hong, S. Zhao, H. Wang, and L. Zhang, "Remaining useful life prediction for lithium-ion battery: A deep learning approach," *IEEE Access*, vol. 6, pp. 50587–50598, Jul. 2018.

[6] P. Voelker, "Trace degradation analysis of lithium-ion battery components," Thermo Fisher Sci., Sunnyvale, CA, USA, Tech. Rep., Apr. 2014. Accessed: Jul. 1, 2020. [Online]. Available: https://www.rdworldonline.com/trace-degradation-analysis-of-lithium-ion-battery-components/

[7] J. S. Goud, R. Kalpana, and B. Singh, "Modeling and estimation of remaining useful life of single cell Li-ion battery," in *Proc. IEEE Int. Conf. Power Electron., Drives Energy Syst. (PEDES)*, Dec. 2018, pp. 1–5.

[8] Q. Badey, G. Cherouvrier, Y. Reynier, M. Duffault, and S. Franger, "Ageing forecast of lithium-ion batteries for electric and hybrid vehicles," *Current Topics Electrochem.*, vol. 16, pp. 65–79, Jan. 2011.

[9] D. Li and L. Yang, "Remaining useful life prediction of lithium battery using convolutional neural network with optimized parameters," in *Proc. 5th Asia Conf. Power Electr. Eng. (ACPEE)*, Jun. 2020, pp. 840–844.

[10] L. Chen, J. Chen, H. Wang, Y. Wang, J. An, R. Yang, and H. Pan, "Remaining useful life prediction of battery using a novel indicator and framework with fractional grey model and unscented particle filter," *IEEE Trans. Power Electron.*, vol. 35, no. 6, pp. 5850–5859, Jun. 2020.

[11] J. Qu, F. Liu, Y. Ma, and J. Fan, "A neural-network-based method for RUL prediction and SOH monitoring of lithium-ion battery," *IEEE Access*, vol. 7, pp. 87178–87191, 2019.

[12] K. Zhang, P. Zhao, C. Sun, Y. Wang, and Z. Chen, "Remaining useful life prediction of aircraft lithium-ion batteries based on F-distribution particle filter and kernel smoothing algorithm," *Chin. J. Aeronaut.*, vol. 33, no. 5, pp. 1517–1531, May 2020.

[13] B. Mo, J. Yu, D. Tang, H. Liu, and J. Yu, "A remaining useful life prediction approach for lithium-ion batteries using Kalman filter and an improved particle filter," in *Proc. IEEE Int. Conf. Prognostics Health Manage. (ICPHM)*, Jun. 2016, pp. 1–5.

[14] X. Xu, C. Yu, S. Tang, X. Sun, X. Si, and L. Wu, "Remaining useful life prediction of lithium-ion batteries based on Wiener processes with considering the relaxation effect," *Energies*, vol. 12, no. 9, pp. 1–17, May 2019.

[15] L. Chen, H. Wang, J. Chen, J. An, B. Ji, Z. Lyu, W. Cao, and H. Pan, "A novel remaining useful life prediction framework for lithium-ion battery using grey model and particle filtering," *Int. J. Energy Res.*, vol. 44, no. 9, pp. 7435–7449, May 2020.

[16] D. Zhang, S. Dey, H. E. Perez, and S. J. Moura, "Remaining useful life estimation of lithium-ion batteries based on thermal dynamics," in *Proc. Amer. Control Conf. (ACC)*, May 2017, pp. 4042–4047.

[17] R. Razavi-Far, S. Chakrabarti, M. Saif, E. Zio, and V. Palade, "Extreme learning machine based prognostics of battery life," *Int. J. Artif. Intell. Tools*, vol. 27, no. 8, pp. 1–22, Dec. 2018.

[18] X. Li, J. Miao, and J. Ye, "Lithium-ion battery remaining useful life prediction based on grey support vector machines," *Int. J. Adv. Mech. Eng.*, vol. 7, no. 12, pp. 1–8, Dec. 2015.

[19] P. Ma, S. Wang, L. Zhao, M. Pecht, X. Su, and Z. Ye, "An improved exponential model for predicting the remaining useful life of lithium-ion batteries," in *Proc. IEEE Conf. Prognostics Health Manage. (PHM)*, Austin, TX, USA, Jun. 2015, pp. 1–6.

[20] Y. Choi, S. Ryu, K. Park, and H. Kim, "Machine learning-based lithium-ion battery capacity estimation exploiting multi-channel charging profiles," *IEEE Access*, vol. 7, pp. 75143–75152, 2019.

[21] Y. Zhang, R. Xiong, H. He, and M. G. Pecht, "Long short-term memory recurrent neural network for remaining useful life prediction of lithium-ion batteries," *IEEE Trans. Veh. Technol.*, vol. 67, no. 7, pp. 5695–5705, Jul. 2018.

[22] S. Hochreiter and J. Schmidhuber, "Long short-term memory," *Neural Comput.*, vol. 9, no. 8, pp. 1735–1780, Nov. 1997.

[23] X. Li, L. Zhang, Z. Wang, and P. Dong, "Remaining useful life prediction for lithium-ion batteries based on a hybrid model combining the long short-term memory and Elman neural networks," *J. Energy Storage*, vol. 21, pp. 510–518, Feb. 2019.

[24] L. Zhao, Y. Wang, and J. Cheng, "A hybrid method for remaining useful life estimation of lithium-ion battery with regeneration phenomena," *Int. J. Appl. Sci.*, vol. 9, no. 9, p. 1890, May 2019.

[25] B. Saha and K. Goebel. *NASA Ames Prognostic Data Repository*. Accessed: Jan. 6, 2020. [Online]. Available: https://ti.arc.nasa.gov/tech/dash/groups/pcoe/prognostic-data-repository/#battery

BENVOLENCE CHINOMONA (Graduate Student Member, IEEE) received the M.S. degree in mechanical engineering from the National Taiwan University of Science and Technology, in 2017. He is currently pursuing the Ph.D. degree in mechanical engineering with National Cheng Kung University. His research interests include signal processing and machine learning algorithms for system performance analysis.

CHUNHUI CHUNG (Member, IEEE) received the Ph.D. degree in mechanical engineering from the State University of New York at Stony Brook, in 2010. He is currently an Associate Professor with the Department of Mechanical Engineering, National Cheng Kung University, Taiwan. His research interests include metal cutting, abrasive machining, computer-aided manufacturing, vibration, and prognostics and health management.

LIEN-KAI CHANG received the Ph.D. degree in mechanical engineering from National Cheng Kung University, Tainan, Taiwan, in 2016. He is currently a Postdoctoral Fellow of the Department of Mechanical Engineering, National Cheng Kung University. His research interests include the design of ultrasonic motors, the fault diagnosis of electric machines, and servo control applications.

WEI-CHIH SU received the Ph.D. degree from the Department of Civil Engineering, National Chiao Tung University, Taiwan, in 2008. He currently works with the National Center for High-Performance Computing, National Applied Research Laboratories. His current research interests include signal processing, the applications of machine learning on the PHM, and defect detection.

MI-CHING TSAI (Senior Member, IEEE) received the Ph.D. degree in engineering science from the University of Oxford, Oxford, U.K., in 1990. He is currently a Chair Professor with the Department of Mechanical Engineering, National Cheng Kung University, Taiwan. He has authored or coauthored more than 127 journal articles and holds more than 122 patents. His research interests include robust control, servo control, motor design, and the applications of advanced control technologies using DSPs. He is a Fellow of the Institution of Engineering and Technology, U.K., and was an Associate Editor of the IEEE/ASME TRANSACTIONS ON MECHATRONICS, from 2003 to 2007, and the Deputy Minister of the Ministry of Science and Technology, Taiwan, from 2016 to 2017.